The Astrophysical Journal, 574:467–476, 2002 July 20

BOUNDARY STRUCTURES AND CHANGES IN LONG-LIVED CORONAL HOLES

S. W. Kahler
Air Force Research Laboratory, Space Vehicles Directorate, Hanscom AFB, MA 01731; stephen.kahler@hanscom.af.mil
and
H. S. Hudson
Solar Physics Research Corporation, ISAS, Sagamihara-shi, Kanagawa 229, Japan; hudson@isass1.solar.isas.ac.jp
Received 2001 September 18; accepted 2002 March 31

ABSTRACT

We report a first systematic morphological study of the boundaries of coronal holes (CHs) as viewed in soft X-ray images from the *Yohkoh* Soft X-Ray Telescope. The special emphasis is on long-lived (several rotations) CHs that extend from the solar polar regions to midlatitudes. As shown earlier, such equatorward extensions tend to show rigid, rather than differential, rotation. Magnetic reconnection must occur at the "closing" boundary, in such a case, to maintain the CH integrity. We find three kinds of CH boundaries in the soft X-ray observations. The majority are generally ragged and not sharply defined; we also find smooth boundaries to occur near a matching-polarity active region (AR), and loopy boundaries to occur near an opposite-polarity AR. In this latter case the loops clearly do not extend far enough to reach another CH but instead end in normal corona. The CH boundaries evolve slowly, and neither large-scale transient X-ray events nor coronal bright points appeared significant factors in long-term CH boundary development. No direct evidence for magnetic reconnection is seen. We compare these results with those expected from current models, derived largely from considerations of heliospheric conditions rather than the detailed appearance of CHs in the low corona.

Subject headings: Sun: corona — Sun: magnetic fields

1. INTRODUCTION

Solar coronal holes (CHs) are large regions of the corona that are magnetically open to interplanetary space (Wang, Hawley, & Sheeley 1996). In X-ray images of the Sun they can be seen as dark voids in unipolar magnetic regions, in contrast to the X-ray emission from the surrounding regions of closed magnetic fields (Zirker 1977). CHs are also observed from the ground as reduced absorption regions in the He λ10830 line (Zirker 1977; Harvey & Sheeley 1979).

At the minimum of the solar activity cycle the Sun is dominated by two polar CHs of opposite magnetic polarity. In the midlatitude regions two kinds of CHs may be observed. The "isolated" CHs are often located near active regions (ARs; Wang et al. 1996) and have an occurrence rate that follows the solar activity cycle (Insley, Moore, & Harrison 1995). The second kind of CH is the "equatorward extension" of a polar CH. Equatorward extensions were prominent during the *Skylab* mission, which occurred in the declining phase of the solar cycle, but their occurrence rate is fairly uniform during periods away from solar maximum (Insley et al. 1995). They also tend to rotate nearly rigidly, in contrast to the isolated CHs, which tend to rotate differentially with latitude, although somewhat more rigidly than the photospheric differential rotation rate (Insley et al. 1995).

The quasi-rigid rotation of the equatorial-extension CHs occurs in the presence of the solar differential rotation, which shears the photospheric fields at the bases of the CHs. Wang & Sheeley (1993) used a source surface model at 2.5 $R_\odot$ to calculate the positions of the open field lines in a configuration consisting of an axisymmetric dipole field and a bipolar AR oriented east-west near the equator. They found that the model CHs corotated with the nonaxisymmetric driver flux. The magnetic field of the outer corona rotated quasi-rigidly with time and forced the open fields of the CH to corotate approximately with it to prevent a windup of coronal field lines that would violate the current-free assumption of the model interior to the source surface. In general, the role of the nonaxisymmetric flux driver is played by midlatitude ARs in which the fields of one polarity of the AR align with the fields of the same polarity of the polar CH. Extensions of polar CHs across the equator can form when the leading polarity of an AR in one hemisphere is aligned in longitude with the trailing AR polarity in the other hemisphere to form a unipolar field region from the pole to the opposite hemisphere.

Maintaining the quasi-rigid CH boundaries in the context of photospheric differential rotation is a current challenge in coronal physics. According to Wang & Sheeley (1993), when a northern-hemisphere positive polarity element, say, of a closed field line enters a CH, "...the flux associated with it becomes open and the connection to the southern-hemisphere element is severed. Since the latter element remains within a closed field region, it must immediately connect to another positive-polarity element. It does so by disrupting a neighboring field-line connection, leaving a nearby negative-polarity element to seek a new partner, and so on. An analogous process occurs when a photospheric flux element crosses from an open into a closed region." In both cases there is a wavelike motion of flux elements exchanging partners without a significant change in the coronal field configuration.

A different scenario was proposed by Fisk, Zurbuchen, & Schwadron (1999a, 1999b), based on a global model of a tilted magnetic dipole with nonradially expanding field lines anchored in a differentially rotating photosphere. The total open magnetic flux at a source surface must remain constant in that model. Field lines are driven by differential rotation in the open regions of the CHs and by coronal magnetic

pressure gradients outside those regions. By undergoing continual episodes of magnetic reconnection with coronal loops at low heliomagnetic latitudes, the field lines progress through the corona back to the opposite CH boundary.

Besides forming the separatrices between large-scale open and closed magnetic fields in the corona, CH boundaries are the crucial regions for theories of the source of the slow solar wind. Perhaps the first idea was that the slow solar wind originates on open field lines within CHs but near the boundaries where the magnetic flux tube expansion is largest (e.g., Wang et al. 1996; Bravo & Stewart 1997; Neugebauer et al. 1998). The appearance of white-light blobs in LASCO observations suggested to Wang et al. (1998) that the slowest and densest solar wind originates in helmet-streamer loops but with a major component still originating from inside CHs near the boundaries. *Ulysses* observations have shown that compared with the fast wind, the parameters of the slow solar wind are highly variable and the composition more biased toward elements of low first ionization potential (FIP; von Steiger et al. 2000). Wang et al. (1996) interpreted this to mean that some open field lines at CH boundaries, which are the source of slow solar wind, will reconnect with adjacent closed field regions to release coronal material with low FIP material. A similar view (Schwadron, Fisk, & Zurbuchen 1999) is that all the slow solar wind originates from reconnection of open flux tubes with closed loops within the context of a recent heliospheric magnetic field model (Fisk et al. 1999a). While the source region of the slow solar wind remains controversial, it appears that the solution to the problem depends on the physics of the magnetic separatrices at the CH boundaries.

Low-latitude CH boundaries have also been suggested as important factors in coronal eruptive events. Webb et al. (1978) found that large-scale *Skylab* X-ray transients preferentially occurred near CH boundaries in general and growing low-latitude CHs in particular. Gonzalez et al. (1996) also found that the inferred source regions of coronal mass ejections (CMEs) giving rise to intense geomagnetic storms were regions of adjacent growing low-latitude CHs, ARs, and source-surface current sheets, denoted with the acronym CHARCS. Similarly, Bravo, Cruz-Abeyro, & Rojas (1998) argued that CMEs were most geoeffective when they were associated with flaring ARs near low-latitude CHs. In a separate study of interplanetary magnetic clouds, Bravo, Blanco-Cano, & Lopez (1999) found that the solar source regions of the clouds nearly always lay close to low-latitude CHs. In his study of *Yohkoh* X-ray blowouts, Bhatnagar (1996) found that they always erupted from or near the boundaries of CHs. With white-light LASCO coronagraph data at the 1996–1997 solar minimum, Lewis & Simnett (2000) found the most active CME region to lie close to the equatorial extension of the northern polar CH. All these authors have suggested that magnetic reconnection between the open fields of the CHs and the adjacent closed fields along the CH boundaries can cause or facilitate some CMEs.

Despite the obvious importance of temporal changes in CH boundaries as a guide to understanding the magnetic reconnection of coronal loops and to determining the source regions of the slow solar wind (Wang et al. 1996; Schwadron et al. 1999), little observational work has been done on the morphology or physics of those changes. Kahler & Moses (1990) studied *Skylab* X-ray images of CH boundaries and found that X-ray bright points (BPs) played an important role in effecting both CH boundary expansions and contractions with size scales of $\sim 2 \times 10^4$ km. Bromage et al. (2000) reported that small-scale changes of the boundary of the "Elephant's Trunk" CH appeared on timescales of a few hours in observations with the Extreme Ultraviolet Imaging Telescope. In those cases sections of the CH appeared to close and reopen. In another examination of the Elephant's Trunk CH, Zhao, Hoeksema, & Scherrer (1999) found that day-to-day variations in the calculated open field regions only roughly matched the day-to-day variations of the 10830 Å CH boundaries. This suggested that not only the changing photospheric fields but also the interactions between the coronal field and plasma flow are responsible for the changing CH boundaries.

The accumulation of nearly 10 yr of solar full-disk X-ray images with good spatial ($<10''$) and temporal (<1 hr) resolution with the Soft X-Ray Telescope (SXT; Tsuneta et al. 1991) on the *Yohkoh* spacecraft now gives us the opportunity to examine CH boundaries in some detail and to address the recent ideas for coronal magnetic reconnection. The best cases in which to look for evidence of significant reconnection are the low-latitude extensions of polar CHs, which are known to show rigid rotation (Zirker 1977; Wang & Sheeley 1993; Zhao et al. 1999). Their largest divergence from differential flow profiles occurs around or above a latitude of 45°, where the rate of change of the rotation profile is largest (Zhao et al. 1999). We select three CHs from the SXT data for this study. We first describe the magnetic structures at the CH boundaries and briefly compare the X-ray and He λ10830 observations of CH boundaries. After an examination of the changes in the CH boundaries, we conclude with a discussion of scenarios for the magnetic reconnection process at the boundaries.

2. DATA ANALYSIS

We examined the entire data base of SXT observations on laser video disks, looking for good cases of midlatitude extensions of polar CHs. Because of the significantly decreased coronal X-ray brightness and more poorly defined CH boundaries around the period of solar minimum in 1996, similar to the 1976 case two cycles earlier (Kahler, Davis, & Harvey 1983), we did not consider CHs from that period. This precluded, for example, the Elephant's Trunk extension of the north polar CH of 1996 (Zhao et al. 1999; Bromage et al. 2000). The three cases of this study are listed in Table 1 and identified here as YCH1, YCH2, and YCH3 (*Yohkoh* Coronal Hole). This nomenclature signifies that we have not made use of other data sets, such as He I λ10830, in defining their boundaries. YCH1 was an equatorward extension of the negative polarity south polar CH observed at approximate Carrington longitudes 90°–150° over Carrington rotations (CRs) 1846–1849 from 1991 September to December. YCH1 is seen prominently in the multilatitude stack plots of Figure 2A of Wang et al. (1996). YCH2 was another equatorward extension of the negative polarity south polar CH, observed at longitudes 40°–80° over rotations 1851–1855 from 1992 January to May. YCH3 was a recent equatorial extension of the negative polarity north polar CH, observed longitudes 160°–190° over rotations 1968–1971 from 2000 October to 2001 January. Judging from their equatorward extensions, YCH2 and YCH3 rotated at the Carrington period of 27.28 days, but YCH1

TABLE 1
TIMES OF OBSERVATION OF PCH BOUNDARIES

Yohkoh Coronal Hole	Longitude (deg)	Carrington Rotation	Dates Used	Major Data Gaps
YCH1	90–150	1847	None	1991 Oct 4–6
		1848	1991 Oct 31–Nov 3	1991 Oct 31 (6 hr); Nov 2 (11 hr)
		1849	1991 Nov 25–26	1991 Nov 27
		1850	1991 Dec 25	1991 Dec 25 (9 hr); Dec 26–27
YCH2	40–80	1851	1992 Jan 27–29	1992 Jan 27 (16 hr)
		1852	1992 Feb 22–24	
		1853	None	1992 Mar 20–22
		1854	1992 Apr 16–19	
		1855	1992 May 13–15	
YCH3	160–190	1968	2000 Oct 13–15	2000 Oct 15 (9 hr)
		1969	2000 Nov 9–11	
		1970	2000 Dec 6–8	
		1971	None	2000 Jan 2–4

rotated with a period of about 26.5 days, moving westward with time.

For each disk rotation of a YCH we selected for observation a 3 or 4 day period of CH passage near central meridian to minimize the projection effects of high coronal loops on the CH boundaries. In general, the divergence of the magnetic fields with height in CHs allows us to determine accurately the locations of CH boundaries when we observe the boundaries within several days of central meridian passage. Image selection was set for one image per hour throughout the day, with typically 15–23 images per day resulting for each YCH of Table 1. For some days or disk passages, the data gaps precluded those times from the study, as listed in Table 1. A total of 29 days of SXT observations were used in the analysis, three of which were limited in data coverage to a half day or less. Accounting for data gaps, the total coverage was about 27 days.

Each YCH was examined by making a movie of image sequences using only the long exposures in a single SXT filter. The thin aluminum (Al.1) filter was used for YCH1 and YCH2 in 1991 and 1992, and because of the loss of the SXT prefilter in 1992, the thicker AlMg filter was used for YCH3 in 2000. The movie-frame field of view was 256×380 pixels, corresponding to $20'.9 \times 31'.0$ in the usual half-resolution with 2×2 pixels, corresponding to $4''.9 \times 4''.9$. The quarter-resolution (QR) images of 4×4 pixels were resized and combined with the half-resolution images in the movies. For studying the details of the YCH boundaries the half-resolution images were significantly better than the QR images and are used in the figures of this work unless otherwise noted. To track the CH boundaries in time, the initial solar pointing of the movie frame was selectable, and the center of the image frame was translated westward through the movie at the rate compensating for solar rotation at the frame center. The brightness table for the images was defined by the standard SXT logarithmic compression to enhance the faint features characteristic of the CH boundaries. Each movie was viewed by stepping through the images as desired. The SXT CH boundaries were compared with those in the daily Kitt Peak National Observatory (KPNO) He λ10830 synoptic maps and with full-disk magnetograms. We used the magnetograms to determine the general magnetic conditions in and around the CHs but not to do detailed comparisons of SXT features with small ($<0'.5$) magnetic features. The goal here was to do a qualitative assessment of CH boundary morphologies, their associations with magnetic field features, and changes in the CH boundaries.

3. CORONAL HOLE BOUNDARY STRUCTURES

A selected SXT image and matching KPNO magnetogram from each of the three recurrent YCHs are shown in Figure 1. The CHs were selected to have boundaries with strong north-south directions, so in the following descriptions we will often differentiate between the basic western and eastern CH boundaries even though the local boundaries may run east-west. While the magnetic fields within CHs are relatively uniform and weak, the appearances and locations of CH boundaries are determined by the fields lying predominantly outside the CHs. In our survey of the CHs we distinguish three basic kinds of boundaries.

3.1. *Diffuse Field Boundaries*

In terms of total lengths the most prevalent kind of boundary is that located in large scale diffuse coronal fields. We find that these diffuse boundaries at low- and midlatitudes are usually ragged, probably reflecting the nonuniformities of the underlying fields, such as the network pattern. Several examples of diffuse CH boundaries are seen in Figure 1. The southwest boundary of the YCH1 runs east to west and lies in a large high-latitude negative-field region. The eastern and western boundaries of both YCH2 and YCH3 are also seen in Figure 1 to lie predominantly in large negative-field regions. Ragged fields were also characteristic of the high south-latitude east-west boundaries that were prominent features of all three observed rotations of YCH1 and CR 1969 of YCH3.

In several notable cases the diffuse boundaries were smooth. In Figure 2 we show two examples of smooth boundaries extending to at least 50° south that persisted throughout a disk rotation. Since in each case we are observing the eastern boundary in the eastern hemisphere, there should be minimal projection effects on the boundaries. This is confirmed by the observation that the locations of the YCH boundaries match those of the KPNO synoptic map of CH boundaries for the corresponding periods. The first example

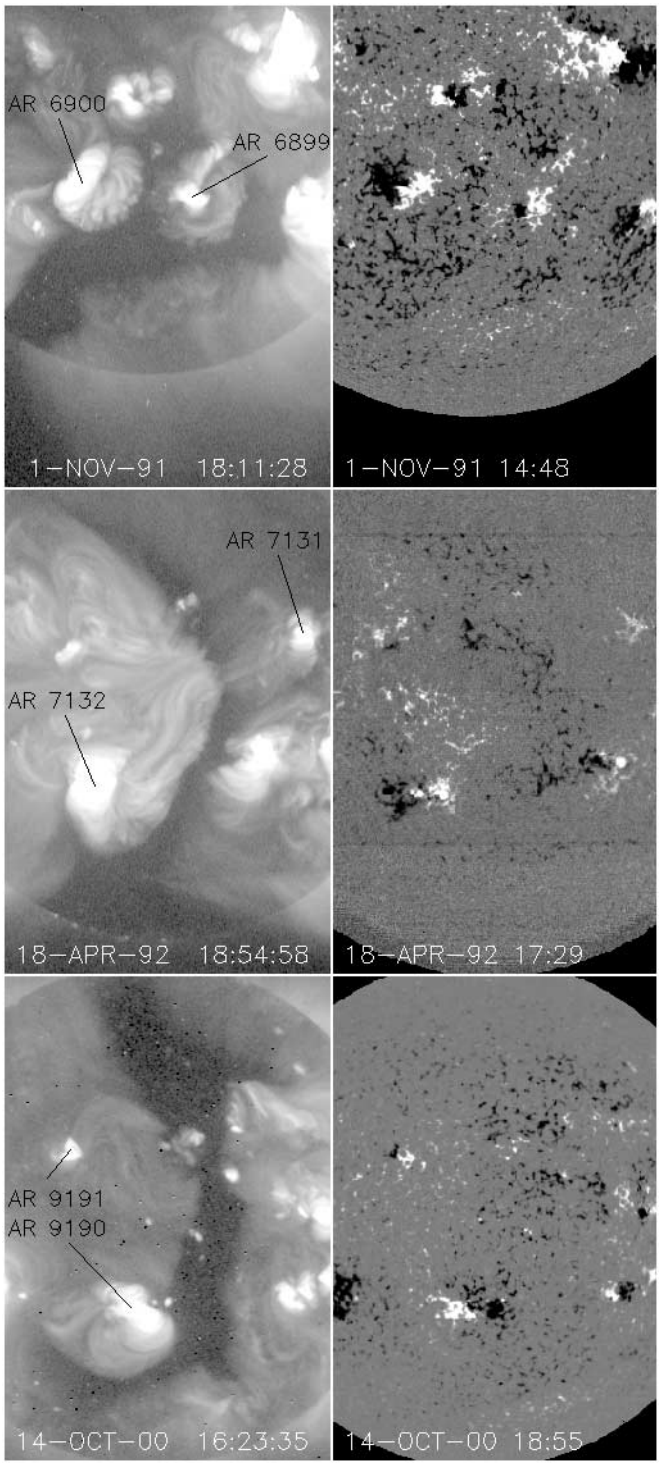

FIG. 1.—SXT images (*left*) and KPNO magnetograms (*right*) near selected central meridian transits of the three YCHs of this study. *Top*: Al.1 image of YCH1 at 18:11 UT on 1991 November 1. *Middle*: Al.1 image of YCH2 observed at 18:54 UT on 1992 April 18. *Bottom*: AlMg image of YCH3 observed at 16:23 UT on 2000 October 14.

occurred during CR 1848 of YCH1 and is shown extending southeast from NOAA AR 6900. The second smooth boundary was observed during CR 1852 of YCH2, although some ripples developed in the northern end late on February 23, as shown in the bottom panels of Figure 2. Another straight and smooth boundary is seen in the narrow channel in the upper part of the February 22–23 images. These boundaries maintained their integrities along smooth arcs with local deviations of less than 10″; even the ripples observed on February 23 deviated by less than 20″ from a smooth arc.

3.2. *Matching-Polarity AR Boundaries*

The second kind of YCH boundary is that formed near an AR magnetic field with a polarity matching that of the YCH field. Figure 3 shows examples of NOAA AR 6901 on 1991 November 1, and NOAA AR 6982 on 1991 December 25. In these cases, as well as that of the leading negative polarity region of NOAA AR 9190 on the southeastern boundary of YCH3 in Figure 1, the boundary with the YCH formed by the AR is bright and smooth. We find that as a general rule the YCH boundaries lying near matching-polarity AR fields show this pattern.

3.3. *Opposite-Polarity AR Boundaries*

The third kind of YCH boundary is that formed near AR fields of polarities opposite that of the YCHs. The right side of Figure 3 shows an example of a complex of ARs with their opposite polarity fields lying along the east-west YCH boundary. Contrary to the second kind of YCH boundary, the opposite-polarity fields are characterized by complexity and multiple loop extensions toward the YCH.

A number of additional examples of opposite-polarity boundaries are found in Figure 1. Both the leading and trailing polarities of NOAA AR 9190 in YCH3 lie on the YCH boundary, with the leading-polarity fields forming a smooth same-polarity boundary and the trailing polarity fields forming the complex loop connections to the YCH. In the YCH2 image the leading opposite polarity fields of NOAA AR 7132 on the southeastern boundary form an arcade of bright loops to connect to the YCH. Another example in the same image is that of the small NOAA AR 7131, which is more than 20° west of the western YCH2 boundary. The opposite-polarity fields of that AR are connected by loops to the western boundary of the YCH. Finally, the 1991 November 1 YCH1 image shows two further examples of NOAA AR 6900 on the eastern boundary and NOAA AR 6899 on or near the western boundary. In the latter case the loops are widely divergent from the leading polarity fields into the YCH boundary fields. The opposite-polarity fields of these ARs directly form the YCH boundaries with loops connecting their fields to the weaker fields that border the YCHs. Those loop connections vary considerably, however, depending on whether the AR is distant from the YCH boundary, as was the case with NOAA AR 7131 of YCH2; lies on the YCH boundary, as were the cases for NOAA AR 9190 of YCH3, AR 7132 of YCH2, and AR 6900 of YCH1; or lies in the YCH, as did AR 6899 in YCH1, all shown in Figure 1.

4. CORONAL HOLE BOUNDARY ACTIVITY

The variations of the YCH boundaries are characterized primarily by slow changes with time and size scales undetectable in successive images from the SXT movies. Figure 4 shows two sequences of narrow longitudinal YCH images over 1 day intervals with approximate 3 hr cadences. These two days were chosen primarily because of their predominant north-south YCH extensions, which allowed us to line up the narrow strips for easy comparison. At the diffuse

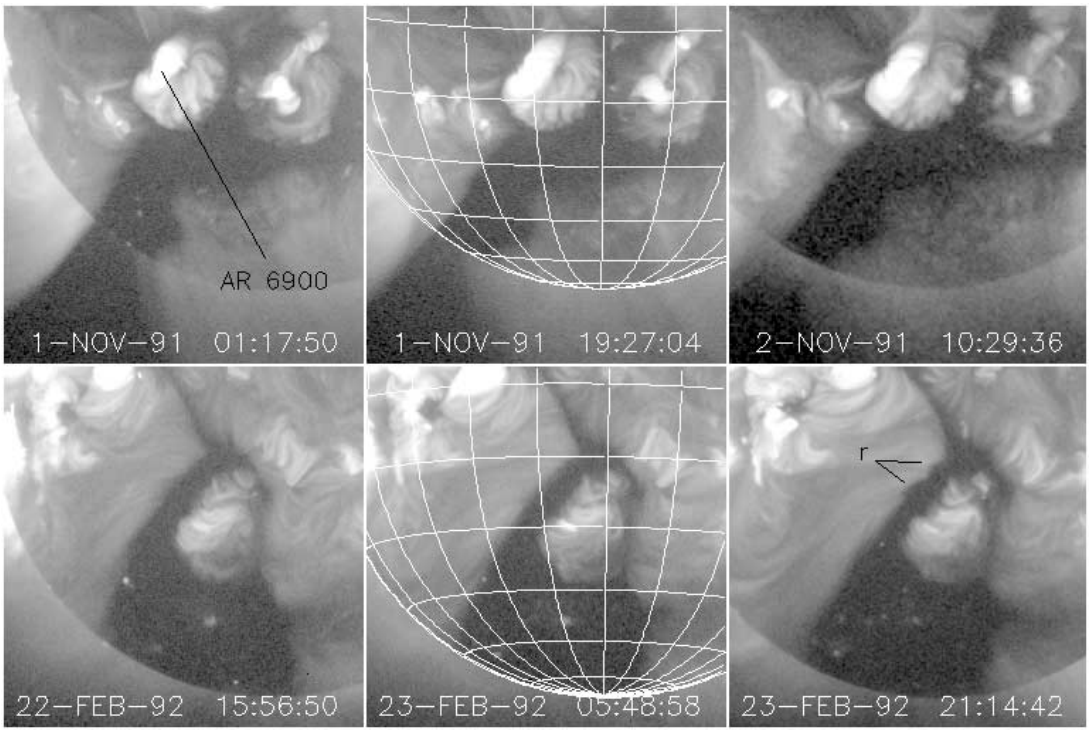

FIG. 2.—*Top*: Three Al.1 images of the southeast boundary of YCH1 during 1991 November 1–2. The last image is QR. *Bottom*: Three Al.1 images of the southeast boundary of YCH2 during 1992 February 22–23. Small ripples that developed are indicated by " r." Contrary to the ragged diffuse YCH boundaries evident in Figure 1, these boundaries were very smooth and straight, extending to about S55° in each case. The solar heliographic coordinate grids on this and other figures indicate every 15° of latitude and longitude.

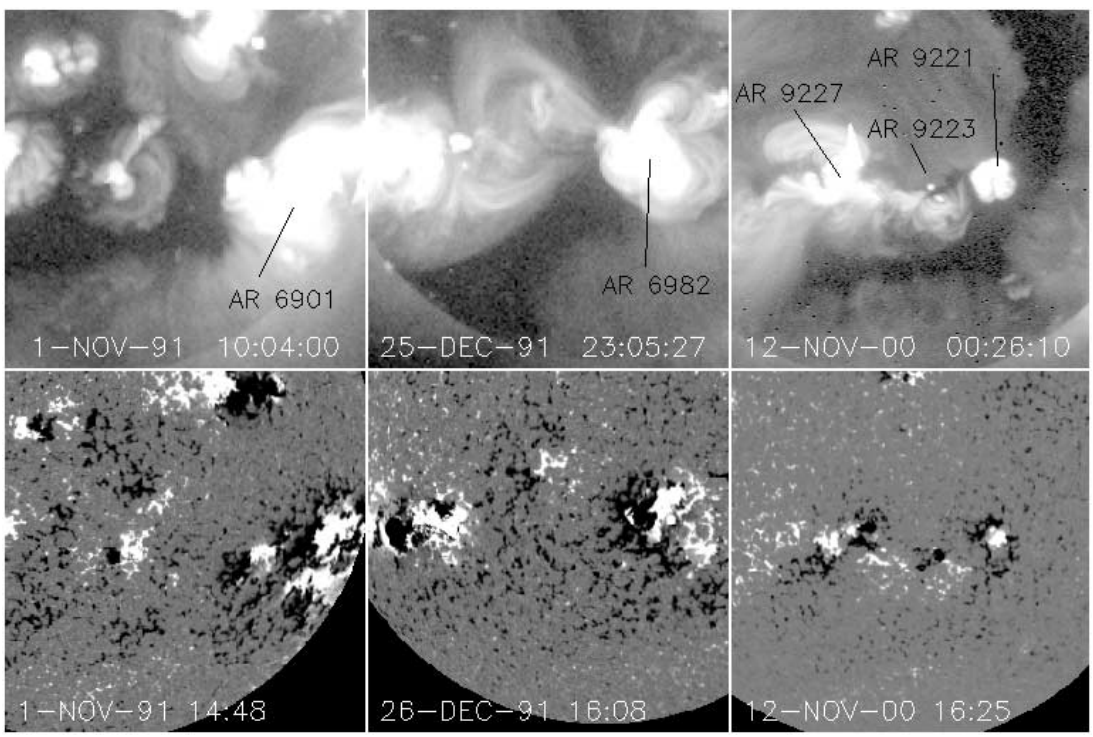

FIG. 3.—*Top*: Examples of ARs at YCH boundaries. *Left*: QR Al.1 image of NOAA AR 6901 on 1991 November 1. *Center*: Al.1 image of NOAA AR 6982 on 1991 December 25. The matching polarity fields of these ARs form smooth, curved bright boundaries of the associated YCHs. *Right*: AlMg image of NOAA AR 9227, AR 9223, and AR 9221 running from east to west along the southeast boundary of YCH3 on 2000 November 12. The opposite polarity fields of these ARs form a complex of loop connections to the YCH. *Bottom*: The associated KPNO magnetograms.

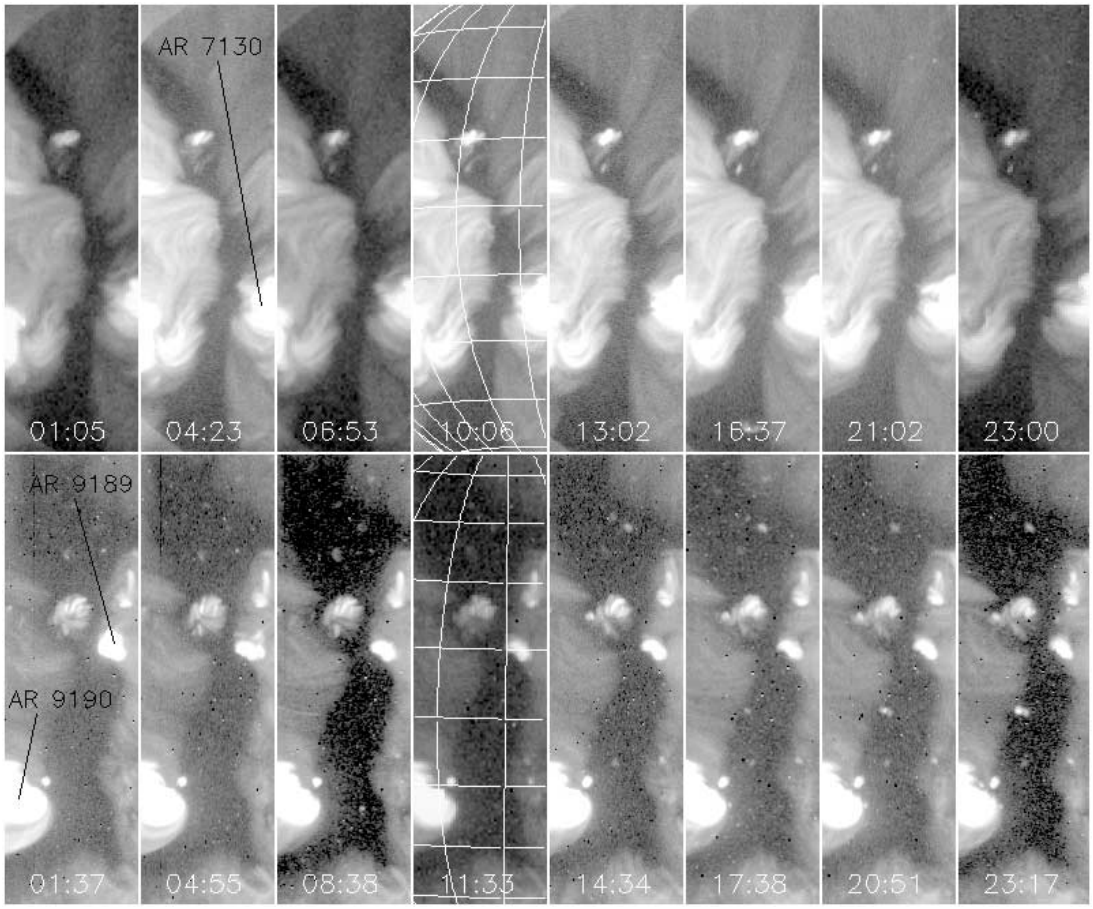

FIG. 4.—Two daily sequences of long north-south YCH passages showing basic slow evolution of the YCH boundaries. In each sequence the frames are centered on a fixed solar longitude, and a solar coordinate grid is placed on one image to indicate locations. *Top*: A sequence of Al.1 images during the 1992 April 16 passage of YCH2. The 01:05, 06:53, and 23:00 UT images are QR. The principal activity consists of loop motions on the diffuse western boundary near the equator, a brightening of a faint loop eastward of the bipolar region in the northern interior part of the YCH, and loop brightenings and/or motions in NOAA AR 7130 on the southwestern boundary, all between 13:02 and 21:02 UT. *Bottom*: A sequence of AlMg images during the 2000 October 13 passage of YCH3. The 11:33 UT image is QR. At 01:37 UT a small eruptive event occurred in AR 9189 on the western boundary, and the bright AR 9190 in the southeast showed brightness variations during the day. In the YCH itself small fluctuations occurred in the bipolar region in the north, and two small bipoles emerged east of that region and near the equator at 17:38 UT, but almost no other activity can be discerned.

boundaries little activity is seen either in these sequences or in the movies with approximately hourly cadences that we examined. Some activity occurs in the regions of strong fields, the ARs and small bipoles in particular, but such activity is also generally seen in similar regions far from CHs.

The smooth and fairly straight high-latitude boundaries of Figure 2 provide another example of the lack of activity at diffuse boundaries. In a typical day no discrete events or changes were observed at these boundaries. Both boundaries made angles of about 50° to the meridian and appeared to be undergoing the strong shearing expected from differential rotation. However, we measured the corresponding angles along the same boundaries during the preceding and following rotations, and in each case the angles were the same to within 5° on the preceding rotations (CRs 1847 and 1851) and only somewhat more sheared to about 65° on the following rotations (CRs 1849 and 1853). The basic conclusion is that at all latitudes where there are no strong field regions, changes in YCH boundaries were rarely perceptible as brightness variations.

This absence of brightness variations also applies to the predominantly east-west boundaries observed at high latitude, as mentioned in § 3 and seen in the 1991 November passage of YCH1, shown in Figures 1 and 3, and in the 2000 November image of Figure 3. At those YCH boundaries the faint loop features of the high latitude coronal structures could be seen apparently rotating eastward in our frame of observation, which followed a fixed solar location centered on a low-latitude point. Thus, we saw little evidence of interactions between those open and closed field regions, as they appeared to rotate differentially past each other.

In the few cases where we clearly see discrete loop variations at YCH boundaries, we can get some insight into the loop lengths and the closed field regions to which the boundary loops are either connecting or disconnecting. In Figure 5 we show three examples of loop variations. The loops that vary in the 2000 January 27 sequence connect the YCH boundary to a region about 30° distant to the east. The loops from the positive polarity fields of the two ARs in the 1992 April 19 period spanned about 15° and underwent a number of brightness changes on that day, but even in those changes it is difficult to determine whether the loops are opening or closing, undergoing reconnection, or simply brightening in place. The connecting loops of the 2000 December 8 period were about 25°–30° in length. Note that 10° in heliographic coordinates equals about 120 Mm.

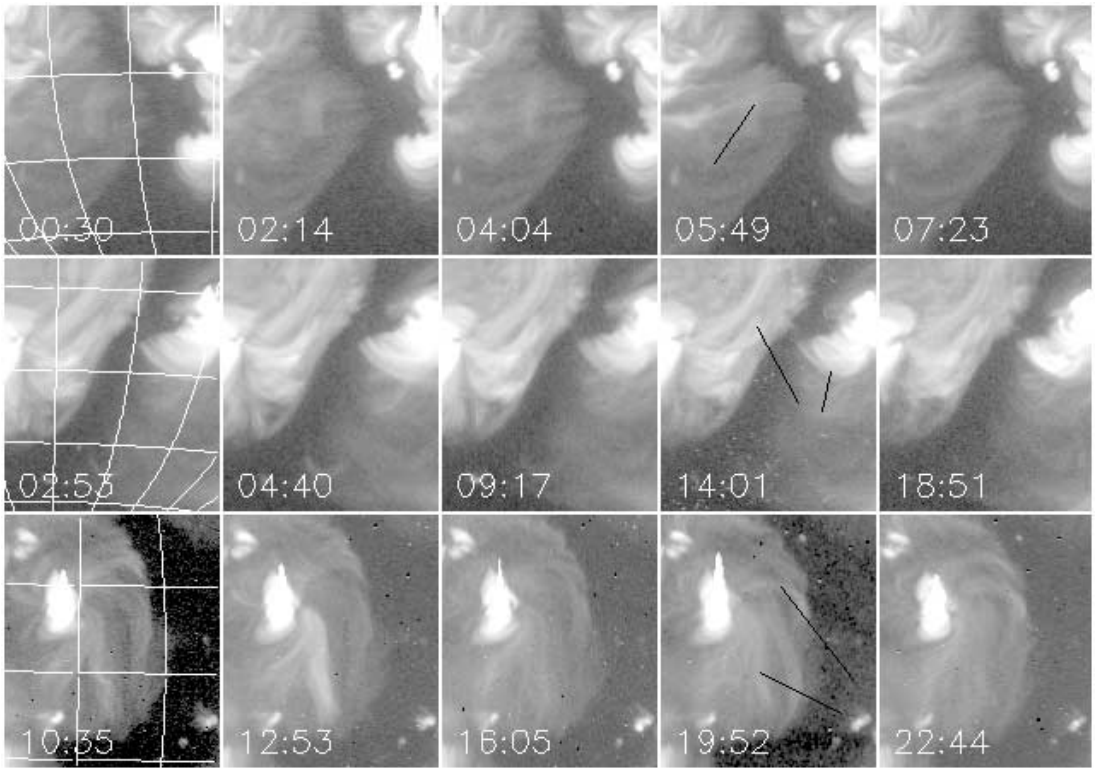

FIG. 5.—Three examples of relatively clear cases of loop variations at YCH boundaries. The solar coordinate grids provide measures of locations and loop lengths. *Top*: Al.1 images of a sequence of loop activity in a diffuse region of the eastern boundary of YCH2 on 1992 January 27. A shifting of loops, indicated by the black line, is obvious only in the last three panels. *Middle*: Al.1 images on 1992 April 19 showing subtle brightness changes in loops connecting the western boundary of YCH2 with NOAA AR 7130 (*black line in west*) and the eastern boundary with AR 7132 (*black line in east*). *Bottom*: AlMg images showing activity of loops connecting AR 9254 (*black line*) with the eastern boundary of YCH3 on 2000 December 8.

The same range of lengths (15°–30°) for CH boundary loops is seen in Figure 1. In YCH1 the lengths of the obvious loop connections of the two ARs in the south are about 10°. Several loop systems are evident in YCH2, some apparently extending from near the equator southward, along a filament channel on the eastern boundary, a distance of 30°. Another loop system extends about 15°–20° from the western boundary to NOAA AR 7131 in the west. In YCH3 a network of loops can be seen extending at least 20° from NOAA AR 9191 in the northern hemisphere to the northeast boundary. In the cases where individual or groups of long-lived or transient loops could be discerned around YCH boundaries, we found that they usually extended directly to the boundaries themselves. In no case did the identifiable discrete loop connections extend from the CH boundary to the boundary of another CH.

In the examination of the YCH boundaries we have looked for cases of large-scale (>10°) eruptive transient events that may have resulted in significant boundary changes (see the discussion of transient CHs in Kahler & Hudson 2001). In the 27 days of observations, we noted four cases of AR eruptions and two eruptions outside ARs. In none of the cases did the transient events appear to produce a change in the YCH boundaries lasting more than about 12 hr. Figure 6 shows the two transients occurring outside ARs. The high-latitude event on 1991 November 3 lay along an east-west neutral line (NL), in which, as discussed above, the features of the closed fields on the polar sides of the NLs appeared to rotate differentially past the YCHs with no obvious interactions between the two field systems. The second event, on 1992 May 15, occurred along the northern part of YCH2, which was probably obscured by the coronal loops at the YCH2 eastern boundary. A transient CH lay along the YCH2 boundary, as shown in the 11:06 UT image. In both cases the appearances of the YCHs showed no evidence of significant long-term (>1 day) changes.

The YCH boundary data were examined for any significant role played by coronal BPs. Very few BPs were observed within or at the boundaries of YCH1 and YCH2, but a number were observed in the YCH3 data. The images of YCH3 of Figure 4 show several BPs both inside the YCH and outside the boundaries, but in no case did we see any evidence of an interaction with larger loop structures. This was also the case with the BPs seen in the YCH3 image of Figure 1. In our survey of the data we found only a single case at 20:21 UT on 2000 November 10 in which a BP in YCH3 at 45° north appeared near the western YCH3 boundary and appeared at the base of a high loop that may have been a westward movement of that diffuse boundary. That was a notable exception, however, to the general lack of any interaction that we found between BPs and YCH boundaries.

5. DISCUSSION

5.1. *Observed CH Boundary Changes and Structures*

Solar-wind studies continue to focus on CH boundaries either as source regions of slow solar wind or as surfaces separating the fast and the slow solar wind flows. If all CH

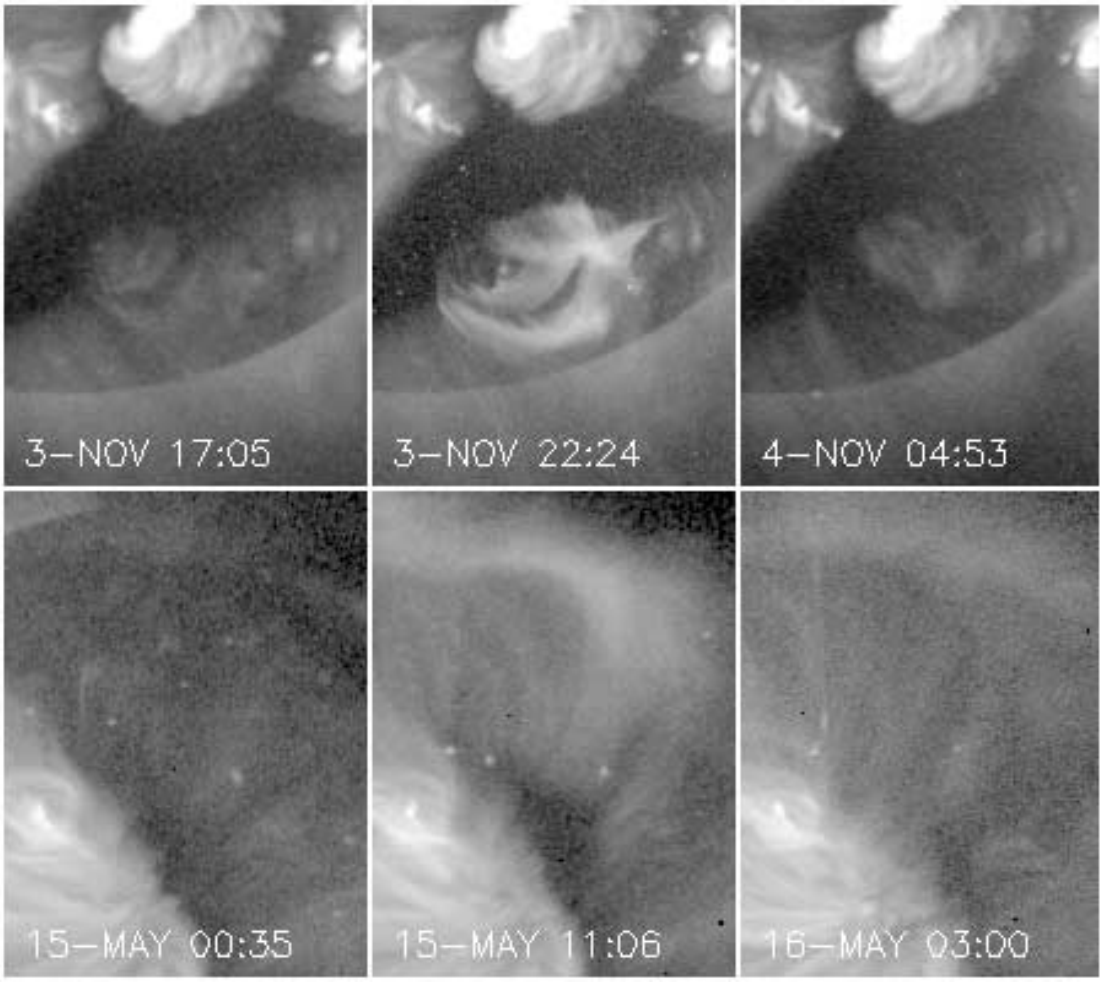

FIG. 6.—Two coronal transients at YCH boundaries. These are the only two cases of transients not involving ARs. *Top*: Al.1 images of a complex eruption that began about 21:00 UT on 1991 November 3 along an east-west part of YCH1. This event did not appear to produce a long-lasting change on the boundary of that region. *Bottom*: Al.1 images of a large transient on 1992 May 15 produced an arcade parallel to YCH2.

boundaries were physically similar, this might be a reasonable approach, but we find that the magnetic structures seen in X-rays at CH boundaries are of three basic types, each of which could produce significantly different kinds of interaction between the adjacent closed and open magnetic fields. The AR fields probably provide the starkest comparison. When the polarities of the adjacent AR fields match those of the CH, a smooth boundary with a sharp X-ray brightness gradient usually results, suggesting minimal interaction between the closed AR fields and the open CH fields. In these ARs we often see loops brightening or flaring and appearing to rise, but this is also the case for most ARs. On the other hand, the magnetic interactions between CH fields and AR fields of opposite polarity are much more complex. There are usually numerous and dynamic bright X-ray loops tracing connections between the two regions of opposite polarity and forming part of the CH boundaries. The dynamic nature is more evident when the CH boundary runs east-west, as seen in several ARs of Figure 3, in which case the proper motions of the AR fields would be a continuous source of shear for the loop system. The loop connections are clearly undergoing continuous changes, as is evident in our SXT movies but difficult to demonstrate in still images such as Figures 4 and 5. Such action is also evident when ARs lie along north-south NLs.

The third kind of CH boundary feature, the diffuse loops, appears to be the most important for solar wind considerations because they comprise the largest part of the boundary lengths. Their evolution is the least apparent to us in the X-ray range, so we must deduce their development based largely on what they do not do or show, as we explore in the next section. While we are far from any model to discuss how solar wind may arise at or near CH boundaries, we suggest that the scenario may very much depend on which CH boundary structures are relevant for any particular observation.

We find no significant role for either large-scale transients or BPs in the evolution of YCH boundaries. The occurrence of large-scale transients along CH boundaries (Bhatnagar 1996) has suggested the possibility that transients play important roles in CH boundary evolution. Webb et al. (1978) found that when X-ray transients occurred near equatorial (isolated) CHs, those CHs were statistically likely to be increasing in area over long timescales. However, a direct connection between transients and long-term (>1 day) CH boundary displacements was not established. In our $\sim$27 days of observations of boundaries of equatorward extensions of polar CHs, we found only six transients on those boundaries, of which four were in ARs and two outside ARs, and none of those could be associated with a

long-term change in the CH boundaries. This result, however, does not preclude the possibility that CH boundaries could play a significant role in the production of CMEs, as Bhatnagar (1996) and Bravo et al. (1999) have argued.

Kahler & Moses (1990) examined CH boundary changes over a 20 hr cumulative period with X-ray images of *Skylab* CH1 and found boundary changes associated primarily with the appearances and disappearances of BPs. Our more extensive survey does not confirm this result, and we conclude that BPs do not represent a characteristic signature of CH boundary activity.

5.2. *Magnetic Reconnection at CH Boundaries*

A major goal of our study was to determine the dynamics of coronal magnetic field lines at CH boundaries. We chose several examples of long-lived low-latitude extensions of polar CHs with nearly rigid rotation as cases in which significant activity should occur to offset the effects of differential rotation. Calculations based on differential rotation rates show that even after a single rotation the extrapolated mid- and high-latitude CH boundaries are displaced several tens of degrees eastward of their observed positions (Wang & Sheeley 1993; Zhao et al. 1999). The problem, therefore, is to explain how the coronal fields change at CH boundaries to effect a rigid rotation of the CH against the effects of differential rotation. *Our basic observational result is that, except at ARs, the processes that maintain the rigid boundaries proceed with no clear signatures in the X-ray images.* The closed fields at CH boundaries are also found to extend at least 10°–20° away from the boundaries but not to terminate at another CH boundary.

Magnetic reconnection at CH boundaries should involve visible changes to the discrete structures making up the boundary. It should also cause transient heating as a result of energy release. Since we do not observe these effects, we next examine the existing models for consistency with our observations. The models currently discussed basically stem from those of Wang & Sheeley (1993) and of Fisk et al. (1999a, 1999b), which differ substantially. These models primarily aim at describing the observed properties of the solar wind flows and interplanetary magnetic fields in the heliosphere. The same field lines must connect through the corona and be rooted in CHs, however, so the models have an obligation to describe what we see in the low corona.

The sketch in Figure 7 is a standard two-dimensional cartoon that illustrates how the CH fields might open and close to allow CH boundary motion. The CH boundary lies in a unipolar region, as observed. An open field line drifting in from the east (left) reconnects with an opposite-polarity open field to form a new closed field line and a U-shaped field line open at both ends. This results in a displacement of the CH boundary and in a heliospheric "heat flux dropout" configuration, a phenomenon only rarely encountered in heliospheric space (Lin & Kahler 1992). The type of reconnection illustrated in Figure 7 changes the total open magnetic flux, because two previously open field lines have now closed. However, this process would be compensated at the other side of the CH where a closed field line becomes two open field lines.

The alternative type of reconnection, namely, between an open and a closed field line, would not have this property. Most CH boundaries consist of relatively small closed loops; we found no cases consistent with loops connecting two CHs. Thus, open/closed reconnection seems more likely to describe the actual physics at the CH boundary. Wang & Sheeley (1993) liken the process to a "wave of reconnection," whereas Fisk & Schwadron (2001) explicitly use a diffusion theory. The loops at the boundaries of the YCHs have three classes, as we have discussed, and their different scales imply that the effective diffusion coefficient must vary substantially with position.

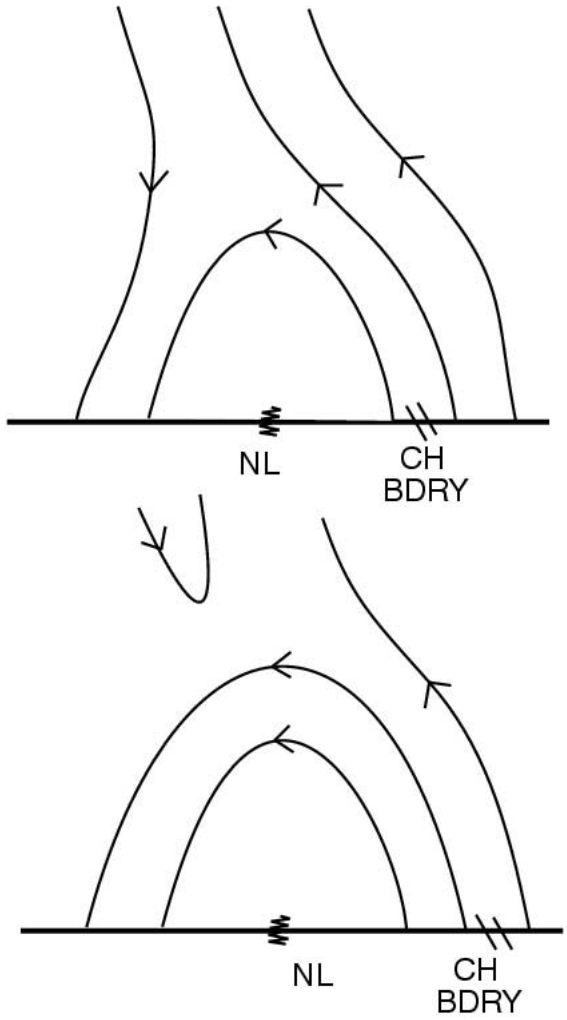

FIG. 7.—Cartoon showing candidate magnetic reconnection scenario at CH boundaries. *Top*: An open positive field line in a CH is convected to the eastern (*left*) CH boundary where it meets a closed field loop. *Bottom*: The open positive field line has reconnected with the open negative-field line. This causes the CH boundary to shift to the right. A disconnected U-shaped field line is also released into the upper corona. NL is the magnetic neutral line.

How do we reconcile our observations, which show little sign of activity or heating at CH boundaries, with the energy release normally expected (as in a flare) from magnetic reconnection? Either open/open or open/closed reconnection should, in principle, deform the field substantially, thus releasing energy as the field relaxes to an unstressed state. The theories and models require this to be happening on the spatial scales of the coronal loops forming the CH boundary, which we find in most cases to be small. We suggest two reasons for the absence of an obvious signature: first, that the reconnection may proceed continuously, without a pronounced energy build-up as in the case of a solar flare,

and second, that the available energy may, in fact, be negligible. In support of the idea of continuous reconnection, rather than a "stick and slip" process, we note that the *Transition Region and Coronal Explorer* observations show that the small-scale solar field (on the supergranular scale) readily reconfigures itself and shows little evidence for braiding that would imply energy storage (Schrijver et al. 1997; Handy & Schrijver 2001).

6. CONCLUSIONS

We have studied the morphology of CH boundaries as seen in *Yohkoh* soft X-ray images, and we find three kinds of X-ray boundaries in these YCHs. The connections between opposite-polarity AR fields and YCH fields are usually composed of bright dynamic loops. Same-polarity AR field boundaries are sharp and bright, while the most common boundaries, formed by loops tracing large-scale ($>10^\circ$) coronal fields, are generally diffuse and ragged. Changes in the boundaries are nearly always subtle and gradual, suggesting that as the boundaries change through magnetic reconnection, the energy of the reconnection process is too small to produce observable X-ray signatures. There does not appear to be an important role for either BPs or large-scale transient events in maintaining the YCH boundaries.

We have interpreted the gradual changes in CH boundaries in terms of magnetic reconnection in the corona, considering the two fundamental possibilities of reconnection between open and closed fields and between open fields only. The former interactions do not allow for variations in the coronal open flux, although that quantity varies by up to a factor of 2 (Sheeley, Knudson, & Wang 2001). The latter would lead to magnetic fields completely detached from the Sun and other fields in the form of closed loops stretched into space, both of which appear to be found rarely in the solar wind. Reconnection between low-lying photospheric magnetic loops and the footpoints of large-scale coronal loops on CH boundaries may play a significant role in facilitating the accommodation of CH boundaries to differential rotation. We suggest that this low-coronal reconnection proceeds continuously, rather than in a "stick-and-slip" manner.

A "Window on Asia" grant from the Air Force Office of Scientific Research supported the work of S. K. We thank T. Kosugi for his hospitality during the stay of S. K. at the Institute of Space and Aeronautical Science. H. H.'s work was supported under NASA contract NAS 98-37334. N. V. Nitta provided valuable assistance with the *Yohkoh* software, and we thank N. Schwadron for helpful discussion. NSO/Kitt Peak data used here are produced cooperatively by NSF/NOAO, NASA/GSFC, and NOAA/SEL.

REFERENCES

Bhatnagar, A. 1996, Ap&SS, 243, 105
Bravo, S., Blanco-Cano, X., & Lopez, C. 1999, J. Geophys. Res., 104, 581
Bravo, S., Cruz-Abeyro, A. L., & Rojas, D. 1998, Ann. Geophys., 16, 49
Bravo, S., & Stewart, G. A. 1997, ApJ, 489, 992
Bromage, B. J. J., et al. 2000, Sol. Phys., 193, 181
Fisk, L. A., & Schwadron, N. A. 2001, ApJ, 560, 425
Fisk, L. A., Zurbuchen, T. H., & Schwadron, N. A. 1999a, ApJ, 521, 868
———. 1999b, Space Sci. Rev., 87, 43
Gonzalez, W. D., Tsurutani, B. T., McIntosh, P. S., & Clua de Gonzalez, A. L. 1996, Geophys. Res. Lett., 23, 2577
Handy, B. N., & Schrijver, C. J. 2001, ApJ, 547, 1100
Harvey, J. W., & Sheeley, N. R., Jr. 1979, Space Sci. Rev., 23, 139
Insley, J. E., Moore, V., & Harrison, R. A. 1995, Sol. Phys., 160, 1
Kahler, S. W., Davis, J. M., & Harvey, J. W. 1983, Sol. Phys., 87, 47
Kahler, S. W., & Hudson, H. S. 2001, J. Geophys. Res., 106, 29239
Kahler, S. W., & Moses, D. 1990, ApJ, 362, 728
Lewis, D. J., & Simnett, G. M. 2000, Sol. Phys., 191, 185
Lin, R. P., & Kahler, S. W. 1992, J. Geophys. Res., 97, 8203
Neugebauer, M., et al. 1998, J. Geophys. Res., 103, 14587
Schrijver, C. J., Title, A. M., van Ballegooijen, A. A., Hagenaar, H. J., & Shine, R. A. 1997, ApJ, 487, 424
Schwadron, N. A., Fisk, L. A., & Zurbuchen, T. H. 1999, ApJ, 521, 859
Sheeley, N. R., Jr., Knudson, T. N., & Wang, Y.-M. 2001, ApJ, 546, L131
Tsuneta, S., et al. 1991, Sol. Phys., 136, 37
von Steiger, R., et al. 2000, J. Geophys. Res., 105, 27217
Wang, Y.-M., Hawley, S. H., & Sheeley, N. R., Jr. 1996, Science, 271, 464
Wang, Y.-M., & Sheeley, N. R., Jr. 1993, ApJ, 414, 916
Wang, Y.-M., et al. 1998, ApJ, 498, L165
Webb, D. F., McIntosh, P. S., Nolte, J. T., & Solodyna, C. V. 1978, Sol. Phys., 58, 389
Zhao, X. P., Hoeksema, J. T., & Scherrer, P. H. 1999, J. Geophys. Res., 104, 9735
Zirker, J. B., ed. 1977, Coronal Holes and High-Speed Wind Streams (Boulder: Colorado Associated Univ. Press)